JOURNAL OF THE AMERICAN WATER RESOURCES ASSOCIATION
Vol. 52, No. 6 AMERICAN WATER RESOURCES ASSOCIATION December 2016

CHARACTERIZING RUNOFF AND WATER YIELD FOR HEADWATER CATCHMENTS IN THE SOUTHERN SIERRA NEVADA[1]

Mohammad Safeeq and Carolyn T. Hunsaker[2]

ABSTRACT: In a Mediterranean climate where much of the precipitation falls during winter, snowpacks serve as the primary source of dry season runoff. Increased warming has led to significant changes in hydrology of the western United States. An important question in this context is how to best manage forested catchments for water and other ecosystem services? Answering this basic question requires detailed understanding of hydrologic functioning of these catchments. Here, we depict the differences in hydrologic response of 10 catchments. Size of the study catchments ranges from 50 to 475 ha, and they span between 1,782 and 2,373 m elevation in the rain-snow transitional zone. Mean annual streamflow ranged from 281 to 408 mm in the low elevation Providence and 436 to 656 mm in the high elevation Bull catchments, resulting in a 49 mm streamflow increase per 100 m (R^2 = 0.79) elevation gain, despite similar precipitation across the 10 catchments. Although high elevation Bull catchments received significantly more precipitation as snow and thus experienced a delayed melt, this increase in streamflow with elevation was mainly due to a reduction in evapotranspiration (ET) with elevation (45 mm/100 m, R^2 = 0.65). The reduction in ET was attributed to decline in vegetation density, growing season, and atmospheric demand with increasing elevation. These findings suggest changes in streamflow in response to climate warming may likely depend on how vegetation responds to those changes in climate.

(KEY TERMS: Sierra Nevada; water yield; normalized difference vegetation index; evapotranspiration.)

Safeeq, Mohammad and Carolyn T. Hunsaker, 2016. Characterizing Runoff and Water Yield for Headwater Catchments in the Southern Sierra Nevada. *Journal of the American Water Resources Association* (JAWRA) 52(6):1327-1346. DOI: 10.1111/1752-1688.12457

INTRODUCTION

The Sierra Nevada mountain range in the western United States (U.S.) has been described as California's water tower. In a Mediterranean climate where much of the annual precipitation falls during the winter, snow-capped mountains serve as the primary source of dry season runoff that supports agriculture, industries, urban, and natural ecosystems. However, increased warming has led to significant reductions in mountain snowpack accumulation and earlier snowmelt throughout the western U.S. (Hamlet *et al.*, 2005; Mote *et al.*, 2005; Harpold *et al.*, 2012). As a result, declines in dry season streamflow (Luce and Holden, 2009; Safeeq *et al.*, 2013), earlier streamflow timing (Stewart *et al.*, 2005; Maurer *et al.*, 2007), and altered flood risk due to a potential increase in peakflow (Hamlet and Lettenmaier, 2007; Tohver *et al.*, 2014; Safeeq *et al.*, 2015a) have been reported across the region. As temperatures continue to warm, much of the region is expected to experience a shift from

[1]Paper No. JAWRA-15-0173-P of the *Journal of the American Water Resources Association* (JAWRA). Received October 9, 2015; accepted July 25, 2016. **Discussions are open until six months from issue publication**.

[2]Assistant Research Scientist (Safeeq), Sierra Nevada Research Institute, University of California, Merced, 5200 N Lake Road, Merced, California 95343; and Research Ecologist (Hunsaker), Pacific Southwest Research Station, United States Forest Service, Fresno, California 93710 (E-Mail/Safeeq: msafeeq@ucmerced.edu).

solid (*i.e.*, snow) to liquid (*i.e.*, rain) phase precipitation (Knowles *et al.*, 2006; Klos *et al.*, 2014; Safeeq *et al.*, 2015b). More precipitation falling as rain instead of snow will affect total snow accumulation and the timing of snowmelt and runoff, potentially leading to lower streamflow in late spring and summer (Berghuijs *et al.*, 2014; Safeeq *et al.*, 2014). However, within a specific climate region, the actual magnitude and timing of streamflow decline will vary based on watershed characteristics, such as hydrogeology and snowpack dynamics (Tague and Grant, 2009; Mayer and Naman, 2011; Safeeq *et al.*, 2013, 2014). Hence, quantitative characterization of streamflow (both magnitude and rate) and water yield from headwater catchments with respect to their physiographic (*e.g.*, elevation, vegetation, soil) and climatic (precipitation and temperature) differences is an essential first step in making predictions about future water availability.

The southern Sierra Nevada is dominated by Mesozoic granite (Parrish, 2006; Frassetto *et al.*, 2011). Udic inceptisols and rock outcrop dominate the higher elevations of the Sierra Nevada (Soil Survey Staff, 2015). Climate and catchment chracteristics in the western slopes of the Sierra Nevada mountain range vary significantly with elevation that ranges from less than 300 to over 4,400 m. While warm foothills (<500 m) receive all of the annual precipitation as rainfall, upper elevations are generally dominated by snowfall (Klos *et al.*, 2014; Safeeq *et al.*, 2015b). The mid-elevations (500-2,500 m) are characterized as the rain-snow transitional zone where precipitation phase shifts between rainfall and snowfall depending on the temperature (Safeeq *et al.*, 2015b). Together, climate gradient and underlying soil/geology dictates the vegetation distribution across the Sierra Nevada mountain range. The warm and dry foothills are dominated by grassland and oak woodland. Mixed conifer forest and alpine shrubland dominate the cold and wet mid- and high-elevations of the Sierra Nevada.

Vegetation plays an important role in determining catchment water budget through various hydrological processes such as interception, infiltration, soil evaporation, and transpiration. In the U.S. alone, forested landscapes occupy 33% of the land area and account for two-thirds of the freshwater supply to 180 million people (Jones *et al.*, 2009). In that regard, effectively managing the forested landscape for maximizing freshwater supply downstream (*i.e.*, water yield) has been a subject of scientific research for decades (Bosch and Hewlett, 1982; Troendle *et al.*, 2010; Robles *et al.*, 2014). Recently, Grant *et al.* (2013) argued for a greater emphasis on managing forests for reducing forest vulnerability to increasing water stress under climate change. This is different from the often-expressed goal of managing forests to maximize water yield for downstream human uses. In theory, water yield is inversely related to the amount of forest cover because of expected declines in interception and transpiration. However, not all studies confirm streamflow gain following forest cover manipulations (*e.g.*, Stednick, 1996; Andréassian, 2004; Biederman *et al.*, 2014, 2015). The underlying mechanism is rather complex (Troendle *et al.*, 2010) and competing hydrologic processes (*e.g.*, interception, transpiration, evaporation, sublimation) may limit the streamflow response (Biederman *et al.*, 2014, 2015; Saksa, 2015). Additionally, spatial and temporal variability in streamflow and water yield is one of the challenging issues in detecting and regionalizing the effects of forest cover on water yield through paired catchment studies (Andréassian, 2004; Brown *et al.*, 2005) which have been lacking for the Sierra Nevada until recently.

In this study, we utilized a unique dataset from the Kings River Experimental Watersheds (KREW) to explore the influence of catchment differences in topography and vegetation on streamflow and water yield. The KREW, a watershed-level, integrated ecosystem project for long-term research on nested headwater streams, is operated by the U.S. Forest Service (USFS) Pacific Southwest Region. Our main objective in this study was to identify the primary (*e.g.*, climate) and secondary (*e.g.*, landscape chracteristics) controls on streamflow and water yield variability in the KREW catchments. We first compared the hydrographs among different catchments and highlight the differences in the context of elevation. We then extracted key hydrologic signatures (HSs) using daily precipitation and streamflow data followed by the derivation of physical catchment descriptors (PCDs). To gain insight, the HSs were analyzed using multidimensional scaling (a multivariate technique to visualize structure of a dataset) and corrrelation techniques. The developed understanding of spatial patterns of streamflow in the KREW catchments will help better evaluate the effects of forest management and climate variability in the headwater streams of the Sierra Nevada.

MATERIALS AND METHODS

Study Catchments

The KREW is comprised of eight primary headwater catchments of the Kings River Basin within the Sierra National Forest. Two additional catchments (P300 and B200), within which six of the eight

primary catchments are nested, were added in 2005/06 (Figure 1). These catchments are clustered into two groups, Providence and Bull. Providence catchments (P300, P301, P303, P304, and D102) range in size from 49 to 461 ha, and have mean elevations ranging from 1,782 to 1,979 m (Table 1). Bull catchments (B200, B201, B203, B204, and T003) range in size from 53 to 474 ha, and have mean elevation ranging from 2,122 to 2,373 m. All catchments but T003 have a dominant southwest aspect, whereas T003 faces primarily southeast. The average slope of KREW catchments ranges from 17 to 27%, with Providence catchments marginally being steeper than the Bull catchments. The drainage density of these catchments ranges from 4.6 to 10.1 km/km^2 and suggests a relativily well developed drainage network in the low elevation Providence catchments (average drainage density = 7.84 km/km^2) as compared to the high

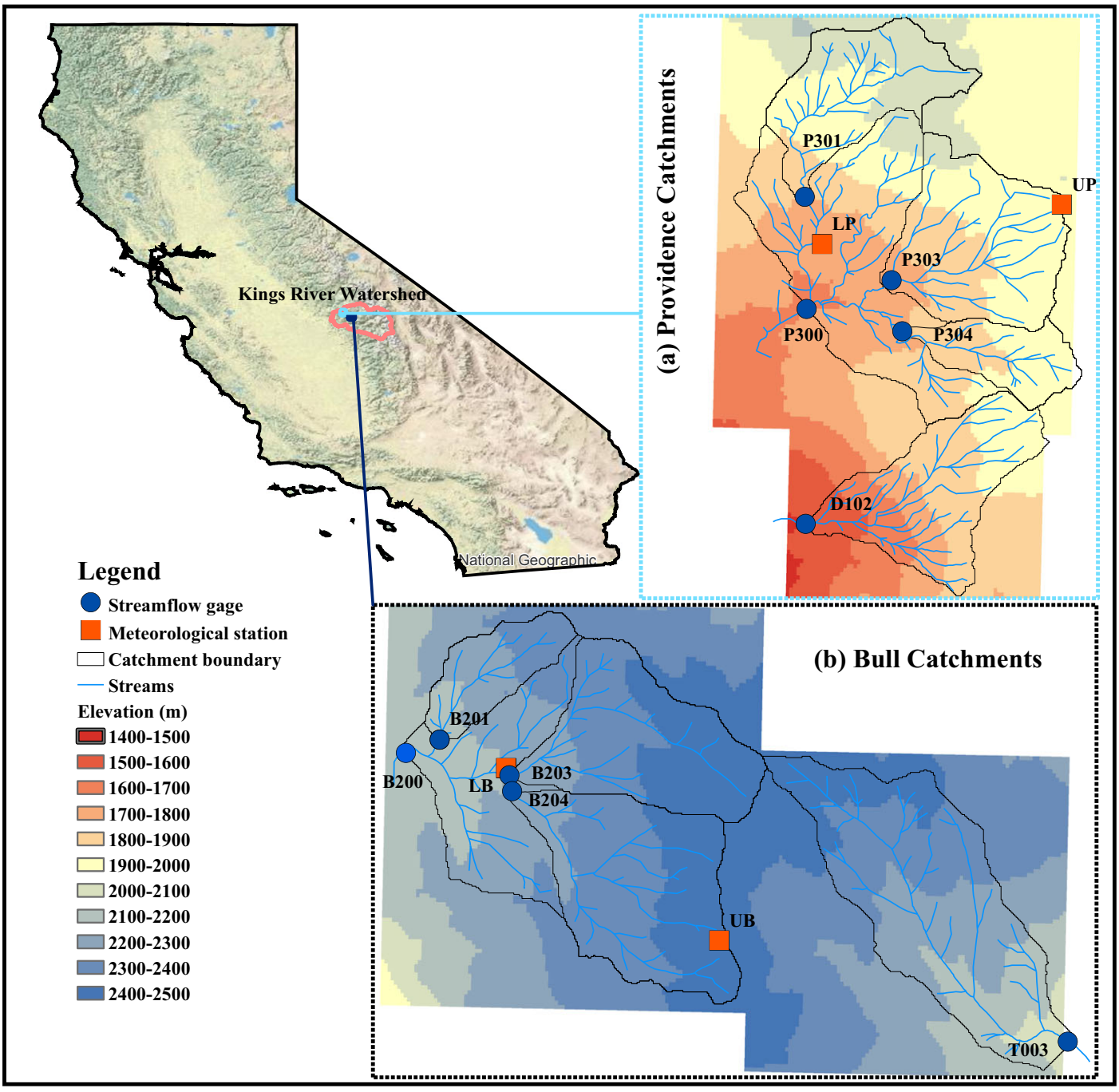

FIGURE 1. Kings River Experimental Watersheds (KREW) Study Area. KREW catchments are grouped into two sites: the lower elevation Providence site (a) and the higher elevation Bull site (b).

TABLE 1. Physical Catchment Descriptors (PCDs) of the 10 KREW Catchments (arranged by elevation).

Catchment	Drainage Area (ha)	Mean Elevation (m)	Relief (m)	Average Aspect (degrees)	Average Slope (%)	Drainage Density (km/km^2)	Mean NDVI (Bare ground[1], %)
Bull							
B203	138	2,373	303	235	18	4.6	0.4627 (4.2)
B204	167	2,365	289	235	17	5.0	0.4854 (2.3)
T003	228	2,289	414	142	24	5.5	0.6304 (1.2)
B201	53	2,257	225	228	18	6.0	0.5413 (1.2)
B200	474	2,122	367	231	18	5.2	0.5084 (2.2)
Providence							
P301	99	1,979	318	208	19	7.4	0.6146 (0.0)
P303	132	1,905	292	233	20	7.4	0.6892 (0.0)
P304	49	1,899	213	249	22	6.9	0.6910 (0.0)
P300	461	1,883	424	223	21	7.4	0.6774 (0.0)
D102	121	1,782	491	246	27	10.1	0.6934 (0.0)

Note: NDVI, normalized difference vegetation index.
[1]Calculated using 30-m U.S. Geological Survey national land cover data: http://www.mrlc.gov/nlcd2011.php.

elevation Bull catchments (average drainage density = 5.26 km/km^2). All catchments have some meadow influnce (Hunsaker *et al.*, 2007). The slightly lower drainage densities in high elevation catchments could be in part related to the presence of more meadows (>2% of land cover). In terms of soil, Shaver dominates the lower elevation Providence catchments with the exception of P301 which is dominated by Gerle-Cagwin. Cagwin soil dominates the higher elevation Bull catchments (Johnson *et al.*, 2011; Hunsaker *et al.*, 2012). The Shaver and Gerle-Cagwin soils in Providence are classified into hydrologic soil group B with rooting depth in the range of 102-203 cm for Shaver and 76-103 cm for Gerle-Cagwin soils. Whereas, Cagwin soil in Bull is classified into hydrologic soil group A with rooting depth in the range of 50-102 cm. The soil parent material for both Providence and Bull catchments is granite (Johnson *et al.*, 2011). Johnson *et al.* (2011) provide detailed information on physical and chemical properties of KREW soil. Land cover is dominated (96-100%) by the Sierran mixed-conifer forest which largely consists of red fir (*Abies magnifica*), white fir (*Abies concolor*), ponderosa pine (*Pinus ponderosa*), Jeffrey pine (*Pinus jeffreyi*), sugar pine (*Pinus lambertiana*), and incense cedar (*Calocedrus decurrens*). Bare ground, mostly rock outcrop in Bull catchments, accounts for 0-4% of the land cover (Table 1). For the KREW experiment, Providence (P301, P303, D102) and Bull (B201, B203, B204) catchments were subjected to vegetation treatments in the form of selective thinning (2012) and/or understory prescribed burning (2013) which may have affected the hydrology of these treated catchments along with portions of P300 and B200. However, because of extremely dry conditions (Figure 2a) in the years during and following the treatments (*i.e.*, 2013 and 2014), the effects of the vegetation treatments may have been very minimal. Additionally, the actual biomass removed from these catchments was below the 20% observed threshold for detecting a hydrologic change (Bosch and Hewlett, 1982; Stednick, 1996; Troendle *et al.*, 2010).

Data Collection

Measurements of stream stage from the individual catchments were made at 15-min intervals, during water years 2004-2014 (except for B200 and P300 where stage measurements began in water year 2006). In 7 of the 10 catchments, stage measurements were taken using a combination of one large (30-122 cm throat width) and one small (8-15 cm throat width) Parshall-Montana flume for measuring high and low flows, respectively. Discharge measurements in catchments P300 and T003 were made using V-notch weirs. For B200, stream stage was monitored using a pressure transducer only and discharge values were estimated using the rating curve method. The discharge measurements for the development of a rating curve for B200 were conducted using the Sontek® FlowTracker Handheld ADV® (FlowTracker, San Diego, California) flow meter across a range of flows. Continuous stream stage recordings were converted to discharge using the stage-discharge relationships across various flow-measuring devices (*i.e.*, flume, weir, and FlowTracker). Across all catchments, the ISCO air bubbler (ISCO™ 730, Teledyne Isco, Lincoln, Nebraska) was used as a primary stage-measurement instrument. Electrical-pulse devices (Aquarod™, Advanced Measurements and Controls, Inc., Camano Island, Washington) and pressure transducers (Telog™, Telog Instruments, Victor, New York) were also installed to provide backup measurements. Manual stage measurements were also conducted during each bi-weekly (unless weather forces a delay) field visits

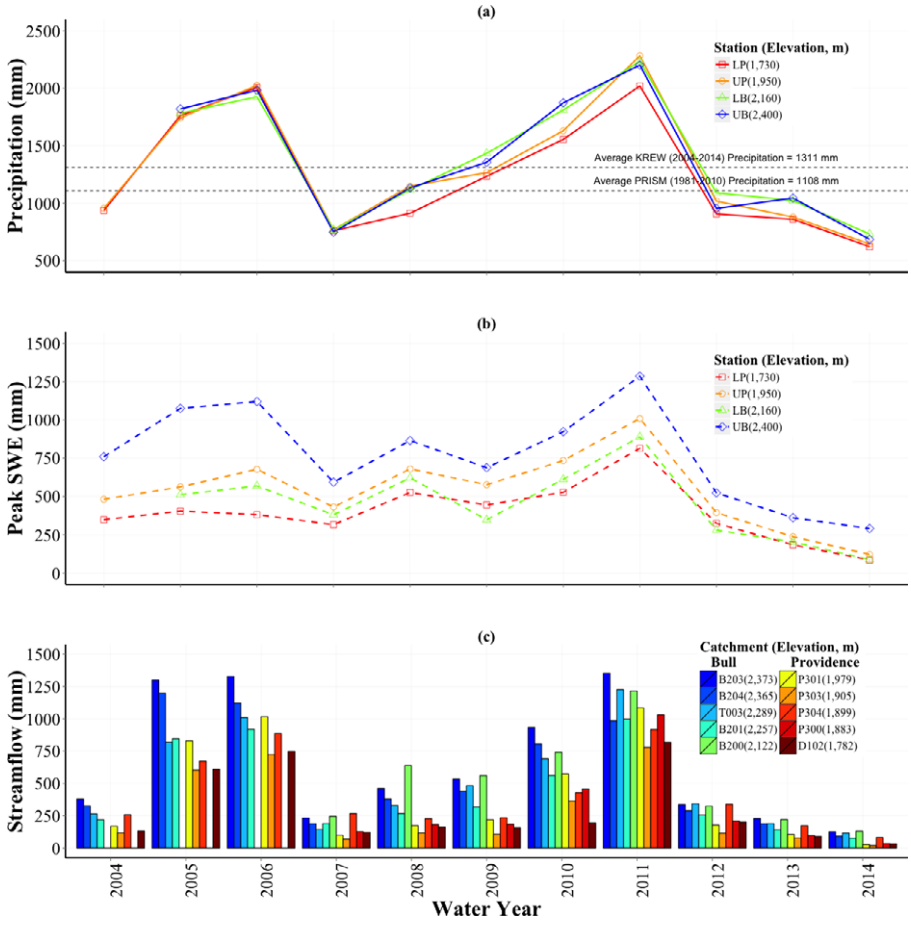

FIGURE 2. Interannual Variability in (a) Annual Precipitation, (b) Peak Snow Water Equivalent (SWE), and Annual Streamflow (c) across the KREW Meteorological Stations and Catchments. Note: The Bull meteorological stations were not active in 2004. Also, P300 and B200 stream gages for measuring discharge were established later. The dotted lines in the top plot (a) show long-term averages for precipitation at the four KREW meteorological stations and for PRISM data (1981-2010).

for data download and regular site maintenance (Hunsaker *et al.*, 2007, 2012). These manual measurements were used during the data quality assessment, and adjustments were made to the digital discharge data if needed. After the quality assessment, all the discharge data were converted from 15-min to equivalent daily unit discharge in mm/day.

The KREW also includes four meteorological stations that were strategically placed to represent lower (Lower Providence: 1,730 m and Lower Bull: 2,160 m) and higher (Upper Providence: 1,950 m and Upper Bull: 2,400 m) elevations within each catchment group (Table 2). All of these meteorological stations are located on the south-facing slopes (aspect ranges between 158° at Lower Providence to 200° Upper Bull) and equipped to monitor precipitation, air temperature, relative humidity, incoming solar radiation, wind speed/direction, and snow depth. These sites are located in open clearings and therefore not subjected to shading from trees or terrain. However, the Lower Bull site is surrounded by rock outcrop that may have some influence on snow accumulation and melt as compared to other sites due to the differences in thermal properties of rock and soil. Precipitation was measured at 15-min intervals using Belfort™ 5-780 shielded weighing rain gages (Belfort Instrument, Baltimore, Maryland) mounted 3 m above the ground on metal frame structures. A nontoxic, propylene-glycol antifreeze was applied to facilitate the snowfall measurements. Similarly, a mineral-based oil layer cover was applied as a barrier to prevent direct evaporation from the collection bucket. The measured precipitation data from these four sites were quality assured against manual measurements taken during each site visit (bi-weekly unless weather forces a delay). We also used digital precipitation measurements taken at a nearby National Atmospheric Deposition Program (NADP: CA28, located a few meters away from the upper Providence Belfort station) and National Oceanic and Atmospheric Administration (NOAA: Huntington, GHCND: USC00044176 and Shaver, GHCND: USR0000CSHA lakes) gages during the quality assurance process. In addition to precipitation gages, all four sites have acoustic snow-depth sensors (Judd Communications™

TABLE 2. Mean and Interannual Variability (SD = standard deviations) in Water Year (WY) Total Precipitation, Precipitation Seasonality (Fall: OND, Winter: JFM, Spring: AMJ, Summer: JAS), and Average Air Temperature (daily) across the Four KREW Meteorological Stations.

			Precipitation Seasonality (mean ± SD) (%)[1]				Daily Temperature (mean ± SD) (°C)[2]			
Station	Elevation (m)	WY Precipitation (mean ± SD) (mm/year)	Fall	Winter	Spring	Summer	Fall	Winter	Spring	Summer
All Years (2004-2014)										
LP	1,730	1,234 ± 514	35 ± 12	48 ± 11	14 ± 7	2 ± 2	6 ± 1	3 ± 1	10 ± 1	18 ± 1
UP	1,950	1,306 ± 539	34 ± 13	49 ± 12	14 ± 7	2 ± 2	7 ± 1	3 ± 1	11 ± 2	19 ± 1
LB	2,160	1,392 ± 522	33 ± 11	47 ± 12	18 ± 8	3 ± 2	4 ± 1	2 ± 1	8 ± 1	16 ± 1
UB	2,400	1,380 ± 549	33 ± 13	49 ± 11	16 ± 8	2 ± 2	4 ± 1	1 ± 1	8 ± 1	16 ± 1
Dry Years (WYs 2004, 2007, 2012, 2013, 2014)										
LP	1,730	817 ± 128	36 ± 16	48 ± 14	12 ± 7	4 ± 2	6 ± 0	4 ± 1	11 ± 0	19 ± 1
UP	1,950	854 ± 148	35 ± 19	47 ± 14	14 ± 8	4 ± 2	7 ± 0	4 ± 1	12 ± 0	19 ± 1
LB	2,160	903 ± 180	32 ± 17	44 ± 12	19 ± 10	5 ± 3	5 ± 0	2 ± 1	9 ± 0	16 ± 1
UB	2,400	858 ± 169	32 ± 20	48 ± 13	16 ± 9	4 ± 3	4 ± 0	2 ± 1	9 ± 0	16 ± 1
Average Years (WYs 2008, 2009)										
LP	1,730	1,074 ± 227	30 ± 3	59 ± 10	10 ± 8	2 ± 1	7 ± 0	3 ± 0	11 ± 1	19 ± 1
UP	1,950	1,207 ± 84	28 ± 6	62 ± 13	9 ± 7	1 ± 1	7 ± 1	3 ± 1	11 ± 1	20 ± 1
LB	2,160	1,275 ± 225	27 ± 8	62 ± 15	10 ± 8	1 ± 1	5 ± 1	1 ± 1	8 ± 1	17 ± 1
UB	2,400	1,245 ± 158	29 ± 6	60 ± 14	10 ± 9	1 ± 1	5 ± 0	1 ± 0	8 ± 1	17 ± 1
Wet Years (WYs 2005, 2006, 2010, 2011)										
LP	1,730	1,837 ± 222	37 ± 9	44 ± 4	19 ± 6	1 ± 1	6 ± 1	3 ± 1	9 ± 1	18 ± 0
UP	1,950	1,920 ± 294	36 ± 8	45 ± 2	18 ± 6	1 ± 0	6 ± 1	2 ± 1	9 ± 1	18 ± 0
LB	2,160	1,939 ± 207	36 ± 7	42 ± 4	21 ± 5	1 ± 1	4 ± 1	1 ± 1	7 ± 2	15 ± 0
UB	2,400	1,970 ± 169	35 ± 7	44 ± 3	20 ± 6	1 ± 1	4 ± 1	0 ± 1	7 ± 2	16 ± 0

Notes: LP, Lower Providence; UP, Upper Providence; LB, Lower Bull; UB, Upper Bull.
[1]Percent of water year total precipitation falling in each season, due to rounding error numbers may not add up to 100.
[2]Average daily temperature for each season.

LLC, Salt Lake City, Utah) installed at 5 m above the ground for measuring snow depth. Monthly snow surveys were also conducted ($n = 5$) by KREW between 2008-2014 using a 4.13-cm internal diameter snow tube (Rickly Hydrological, Inc., Columbus, Ohio). A multiplier of 74.737 cm/kg was used to convert the measured mass of snow (kg) in the snow tube to snow water equivalent (SWE) (cm). We then established regression models for Upper Providence and Upper Bull sites ($R^2 > 0.82$) by relating the measured average snow depths with average SWEs from the snow surveys. The established regression model was then used to convert the digitally measured snow depths from acoustic snow depth sensors to SWE. Snow surveys were not performed at Lower Providence and Lower Bull sites. Hence, the regression equations from the upper elevation sites were used for converting the digital snow depth measurements to SWE at lower elevation sites.

Physical Catchment Descriptors

We extracted seven descriptors to help distinguish the differences in physical catchment characteristics (Table 1). These descriptors include drainage area, elevation, relief, aspect, slope, drainage density, and normalized difference vegetation index (NDVI). The topographic descriptors (*i.e.*, drainage area, elevation, relief, aspect, and slope) were derived using a 30-m digital elevation model obtained from U.S. Geological Survey repository (available online: http://nationalmap.gov/viewer.html). The drainage density parameters were calculated by overlaying the detailed stream network layer, digitized from U.S. Geological Survey topographic maps (Heather Taylor, USFS, personnel communication), on each catchment boundary. Differences in vegetation among the catchments were represented by the Moderate Resolution Imaging Spectrometer (MODIS) 250-m NDVI data (MYD13Q1 version 5). The raw NDVI values were filtered using quality assurance flags and then averaged for the 2004-2014 water years. The temporally averaged NDVI values were intersected with the catchment boundary layer to extract the mean catchment NDVI values.

Hydrologic Signatures

We extracted HSs using precipitation and streamflow data to characterize hydrologic behavior of the catchments. The relevant HSs describing low,

medium, and high flows, groundwater, and climate dependencies were primarily selected from a larger list of possible indices described in hydrologic literature (Kadioglu and Sen, 2001; Olden and Poff, 2003; Baker *et al.*, 2004; Stewart *et al.*, 2005; Yadav *et al.*, 2007; Zheng *et al.*, 2009). The selected HSs are described below.

Runoff Ratio. Runoff ratio (%) is defined as the ratio of catchment discharge to precipitation. The long-term average annual runoff ratio has been used as a metric of water balance separation between discharge and evapotranspiration when assuming no net change in storage (Olden and Poff, 2003; Yadav *et al.*, 2007; Sawicz *et al.*, 2011; Hunsaker *et al.*, 2012). A runoff ratio of 50% indicates that the catchment discharge is the same as the catchment evapotranspiration. A runoff ratio more (less) than 50% indicates that the catchment discharge exceeds (falls behind) the catchment evapotranspiration. Although in theory, runoff ratio can be calculated on any time-scale of interest (*i.e.*, monthly, seasonal, and annual), estimation of runoff ratio at a monthly time scale was not possible for KREW catchments with a Mediterranean climate where the total precipitation during summer months is often zero. For this reason we have only estimated the runoff ratio at annual time scales for 2004-2014.

Climate Elasticity. Climate elasticity of discharge (ε) has been used to describe the sensitivity of a catchment's discharge to changes in precipitation and/or temperature (Schaake, 1990; Sankarasubramanian *et al.*, 2001; Fu *et al.*, 2007; Safeeq and Fares, 2012) and to seperate the individual effects of climate and vegetation on hydrologic response (Zhao *et al.*, 2010). However, the estimation of climate elasticity using the method as proposed by Schaake (1990) and later revised by Sankarasubramanian *et al.* (2001) requires long-term data to avoid numerical instability (Zheng *et al.*, 2009). In this study, we used the revised climate elasticity for a small sample size as proposed by Zheng *et al.* (2009). The revised climate elasticity can be given by:

$$\frac{(Q_i-\bar{Q})}{\bar{Q}}=\varepsilon\frac{(X_i-\bar{X})}{\bar{X}} \quad \text{where } i=1,2,3,\ldots,n \text{ years} \tag{1}$$

where Q_i is discharge for year i, $\bar{Q}$ is the average discharge over n years, X_i is the climate factor (*e.g.*, precipitation or temperature) for year i, $\bar{X}$ is the n year average value of the climate factor. The elasticity of streamflow ε can be estimated as the linear regression coefficient between $(X_i-\bar{X})/\bar{X}$ and $\frac{(Q_i-\bar{Q})}{\bar{Q}}$ using the least squares estimator as:

$$\varepsilon=\frac{\bar{X}}{\bar{Q}}\times\frac{\sum_{i=1}^{n}(X_i-\bar{X})(Q_i-\bar{Q})}{\sum_{i=1}^{n}(X_i-\bar{X})^2}=\rho_{x,Q}\times C_Q/C_X \quad \text{where } i=1,2,3,\ldots n, \text{ years} \tag{2}$$

where $\rho_{x,Q}$ is the correlation coefficient between X and Q; C_X and C_Q are coefficients of variation of X and Q, respectively. Finally, based on the water balance and Budyko hypothesis (Zheng *et al.*, 2009):

$$\varepsilon_P+\varepsilon_{ET_o}=1 \tag{3}$$

where ε_P and ε_{ET_o} are the precipitation and potential evapotranspiration elasticity of discharge, respectivily. As noted by Zheng *et al.* (2009), this complementry relationship between ε_P and ε_{ET_o} may not hold to be true for all catchments due to lack of consideration for changes in storage in the Budyko hypothesis.

Baseflow Magnitude and Recession. Baseflow index (BFI) and recession constant (k) have been used to characterize the drainage efficiency of a catchment. The BFI is defined as the ratio of baseflow, the component of streamflow that can be attributed to groundwater discharge, to total streamflow (Wolock, 2003). Over the years, multiple algorithms have been developed to calculate BFI (*e.g.*, Institute of Hydrology, 1980a,b; Arnold *et al.*, 1995; Arnold and Allen, 1999; Kroll *et al.*, 2004; Eckhardt, 2005). However, for the purpose of this study, BFI values were calculated using the program described in Wahl and Wahl (1988, 1995). The BFI program is based on the N-day non-overlapping smoothed minima approach (Institute of Hydrology, 1980a,b; Wahl and Wahl, 1988). The estimated BFI values can be quite sensitive to the choice of N (Wahl and Wahl, 1995; Miller *et al.*, 2015). However, we did not perform any sensitivity or optimization analysis for N, since our focus was to characterize relative differences among catchments rather than on the actual BFI value. A default suggested value of $N = 5$ was used (Wahl and Wahl, 1995).

Baseflow recession rates were analyzed using the method of Vogel and Kroll (1992). To avoid the effects of precipitation and snowmelt on recession rates, only recession segments lasting 10 days or longer were selected. The beginning of the recession (inflection point) was identified following the method of Arnold *et al.* (1995). As suggested by Vogel and Kroll (1992), daily flow values were smoothed using a three-day moving average window and only accepting pairs of

receding flow (Q_t, Q_{t-1}) when $Q_t > 0.7Q_{t-1}$ to avoid spurious observations. The recession constant k was calculated as:

$$k = exp\left[\frac{1}{m}\sum_{t=1}^{m}\{\ln(Q_{t-1} - Q_t) - \ln[0.5(Q_t + Q_{t+1})]\}\right] \quad (4)$$

where m is the total number of pairs of consecutive daily flow Q_t and Q_{t-1}, at each site. Similar to BFI, several methods exist for recession analysis and there is a considerable debate on appropriate techniques for recession analysis (Tallaksen, 1995; Vogel and Kroll, 1996; Smakhtin, 2001; Sujono *et al.*, 2004; Posavec *et al.*, 2006). Estimates of k are comparable using some techniques (Sujono *et al.*, 2004; Safeeq *et al.*, 2014) but not others (Vogel and Kroll, 1996). Safeeq *et al.* (2013) found a strong correlation between the estimates of k and catchment subsurface geologic/aquifer characteristics and used k as a metric for describing groundwater influence on hydrologic response in the western U.S. streams. This gave us confidence in not only the method we used for estimating k but also using the k for characterizing the relative differences in subsurface properties among the selected catchments.

The BFI and k are inversely related and influenced by the degree of groundwater influence, both in terms of magnitude and subsurface flow path length. Catchments with higher groundwater influence and longer flow paths have higher BFI and slower recession (*i.e.*, lower k values) as compared to quick flow dominated catchments (Safeeq *et al.*, 2013).

Slope of the Flow Duration Curve. The flow duration curve (FDC), a cumulative frequency **curve** that shows the percent of time a specified discharge value was equaled or exceeded during a given period, was derived for each catchment using daily discharge. The slope of the FDC can be used as a metric of catchment hydrologic characteristics. A higher slope value indicates quick flow and represents rainfall dominated catchments with flashy hydrographs and very little ability to sustain low flows during dry seasons due to a lack of surface (*i.e.*, snowpack) and subsurface (*i.e.*, soil and groundwater) storage. In contrast, a low slope value indicates groundwater and snowmelt dominated catchment with damped quick flow response and sustained low flows during dry seasons. Following Sawicz *et al.* (2011), the slope of the FDC was calculated between 33rd and 66th flow percentiles which represents the relatively linear part of the FDC (Yadav *et al.*, 2007; Zhang *et al.*, 2008).

Magnitude, Timing, and Frequency of Flow. Annual one-day minimum, mean, and maximum discharge were used to characterize the selected catchments in terms of flow magnitude. In addition to these, percentile-based (5th, 25th, 75th, and 95th) flow magnitude and cumulative flow over each season (fall, winter, spring, and summer) and water year were also analyzed and used as signatures. Timing of flow dates were defined using the center of mass of annual flow (CT). A threshold-based approach was used to calculate the frequency of a discharge exceeding a given threshold. For this purpose, we calculated stream dry days (DD) as the number of days in a water year when flow on a given day was less than the 7Q10 (the lowest 7-day average flow that occurs on average once every 10 years). Similarly, low pulse (LP) and high pulse (HP) counts (Olden and Poff, 2003) were defined and calculated as the number of days in a water year when flow on a given day was less than 25% and higher than 200% of the mean, respectively.

Precipitation-Streamflow Relationship. Predictive linear models of water year streamflow (Q) using precipitation (P) were developed as:

$$Q = aP + b, \quad (5)$$

where a is the slope (mm/mm) and b is the y-intercept of the regression line. The x-intercept or in this case P-intercept ($-b/a$) can be used as a metric for precipitation threshold for each catchment below which, on average, no streamflow would be predicted. The regression coefficient a was used to infer the responsiveness of streamflow to a unit increase in precipitation beyond the initial threshold (*i.e.*, $-b/a$).

Statistical Analysis

To understand the relationship between PCDs and HSs in space, Pearson's product-moment correlations were performed. The seven parameters of PCDs and eight parameters of HSs were used for the correlation analysis (Table 3). We have restricted the correlation analysis to eight not time-series HSs (with the exception of annual streamflow, runoff ratio, and BFI) to reduce dimensionality of the correlation matrix. Although the choice of HSs for correlation analysis is somewhat subjective, the selected eight HSs represent a range of hydrologic regime types that are relevant for guiding and forming hypotheses for future analyses. We used one-way ANOVA and Welch Two Sample t-test to evaluate significant differences between groups (p-value less than 0.10).

We also used a nonparametric, multidimensional scaling (N-MDS) on Euclidean distance, ordination approach to compare the catchment similarity. The

TABLE 3. Values of Hydrologic Signatures (HSs) for the 10 KREW Catchments. Values are based on 11 years for all catchments except P300 and B200 which are based on 8 years of data. Average values over the record length are reported for the first 18 signatures that are time series in nature.

Signature	Signature Description	Statistical Analysis[1]	Units	Catchment									
				B203	B204	T003	B201	B200	P301	P303	P304	P300	D102
Q_{min}	Minimum streamflow	*N*	mm	0.08	0.11	0.19	0.12	0.10	0.03	0.03	0.36	0.05	0.06
Q_{max}	Maximum streamflow	*N*	mm	14.26	11.95	8.46	9.13	17.73	10.04	8.22	6.63	8.43	10.09
Q_{mean}	Mean streamflow	*N*	mm	1.80	1.50	1.40	1.19	1.40	1.11	0.77	1.12	0.79	0.81
DD (Q < 7Q10)	Frequency of stream dry days	*N*	days	5	2	1	4	18	12	1	7	6	3
HP ($Q > 2^* Q_{mean}$)	Frequency of high streamflows	*N*	days	58	55	47	46	55	62	53	25	53	49
LP ($Q < 0.25^* Q_{mean}$)	Frequency of low streamflows	*N*	days	130	125	64	75	107	124	107	6	91	97
Q_5	Fifth percentile streamflow	*N*	mm	0.13	0.16	0.27	0.18	0.15	0.07	0.06	0.39	0.09	0.08
Q_{25}	Twenty-fifth percentile streamflow	*N*	mm	0.28	0.27	0.43	0.32	0.30	0.17	0.11	0.58	0.22	0.18
Q_{75}	Seventy-fifth percentile streamflow	*N*	mm	1.89	1.40	1.59	1.38	1.62	1.40	1.00	1.36	1.13	1.14
Q_{95}	Ninety-fifth percentile streamflow	*N*	mm	8.22	7.47	5.26	4.72	4.94	4.23	2.84	2.77	2.28	2.41
CT	Streamflow timing	*N*	days	198	208	191	185	186	185	183	181	174	172
Q_{Fall}	Fall streamflow	*N*	mm	45	33	52	46	48	32	20	64	38	32
Q_{Winter}	Winter streamflow	*N*	mm	107	60	90	90	126	99	80	97	85	108
Q_{Spring}	Spring streamflow	*N*	mm	456	399	305	260	290	250	164	179	143	137
Q_{Summer}	Summer streamflow	*N*	mm	48	54	64	39	47	25	17	67	24	21
Q_{Annual}	Annual (water year) streamflow	*NP*	mm	656	547	510	436	511	407	281	408	290	298
Baseflow index (BFI)	Extent of ground- and surface-water interaction	*NP*	%	68.2	68.1	76.1	73.3	54.7	71.6	74.3	88.1	60.0	76.0
Runoff ratio (RR)	% Precipitation that becomes streamflow	*NP*	%	42.9	35.8	33.4	28.4	37.1	25.9	17.7	29.4	20.5	19.7
Slope of the FDC	Streamflow variability	*P*	—	−4.04	−3.25	−2.58	−2.29	−3.35	−3.69	−3.71	−1.85	−3.63	−3.33
Climate elasticity	Responsiveness of streamflow to precipitation	*P*	—	1.83	1.79	1.86	1.91	1.64	2.31	2.38	1.62	2.55	2.13
Recession constant (k)	Extent of ground- and surface-water interaction	*P*	/day	0.037	0.031	0.027	0.033	0.038	0.036	0.031	0.014	0.032	0.027
P-*Q* slope (a)	Responsiveness of streamflow to precipitation	*P*	mm/mm	0.888	0.724	0.703	0.615	0.638	0.740	0.528	0.519	0.617	0.499
P-intercept ($-b/a$)	Precipitation threshold for streamflow	*P*	mm	614.27	597.28	625.97	642.91	462.59	719.61	737.36	484.71	687.13	673.92

Notes: FDC, flow duration curve.

[1]*N* indicates parameters which were used in nonparametric, multidimensional scaling (N-MDS) analysis. *P* indicates parameters for which Pearson's product moment correlations were calculated.

N-MDS scaling is a multivariate technique that aims to reveal the similarity or dissimilarity in a dataset by first reducing the dimensionality of dataset and then plotting the data points to one- or two-dimensional space. Catchments that have very similar hydrologic response (as measured by HSs or any other metrics) will appear as points near each other whereas catchments that have very different hydrologic response will be further away from each other on the plot. The difference in the grouping of points can be analyzed for statistical significance based on categorical factors. The extracted HSs were rearranged via an iterative optimization procedure to minimize stress (a measure of dissimilarities) across sites or time periods in a two-dimensional (2D) plot (Kruskal, 1964). Proximity of points in the 2D plot indicates a higher degree of similarity and vice versa. For this analysis, we have only selected the 18 signatures that were time-series in nature (Table 3). Analysis of similarity (ANOSIM) was performed to statistically test the null hypothesis of no difference among groups of descriptors. The ANOSIM is a nonparametric procedure analogous to analysis of variance (ANOVA) that tests differences in distance in the ordination space of previously defined groups against random groups (Arismendi *et al.*, 2013). The ANOSIM uses R statistics, with value ranging between -1 (more similarity between groups than within groups) and 1 (more dissimilarity between groups than within groups), along with estimated probability (p-value) of rejecting the null hypothesis. Since many of the PCDs were cross-correlated (as discussed later) with elevation, we have used the elevation or Providence *vs.* Bull as one of the primary grouping variables for N-MDS. We also used precipitation (average, dry, and wet years) as the secondary grouping variable to explore the effect of climate variability on catchment hydrologic similarity.

RESULTS

Total water year precipitation measured across the four meteorological stations ranged over three-fold among different years (Figure 2a). On average over 90% of the total annual precipitation across all meteorological stations occurred between October-April (Figure 3a). The increasing rate of precipitation with station elevation varied from zero to as much as 50 mm/100 m in different years. However, as noted by Hunsaker *et al.* (2012), we found no statistically significant difference in annual precipitation (one-way ANOVA, $p = 0.89$) among the different meteorological stations despite their altitudinal differences. Based on the long-term (1981-2010) precipitation anomaly from PRISM (Daly *et al.*, 1994), water years 2004, 2007, 2012, 2013, and 2014 can be characterized as below normal or dry, 2008 and 2009 can be characterized as normal or average, and 2005, 2006, 2010, and 2011 can be characterized as above normal or wet precipitation years. As mentioned previously, this classification of average, wet, and dry years were based on the recent (1980-2010) climatology that may or may not hold true for longer climatological time period. On the extreme ends, total precipitation during wettest (2011) and driest (2014) water years in the study period was about 197% and 61% of the PRISM normal, respectively (Figure 2a). Despite the strong interannual variability, the difference in seasonal distribution of annual precipitation (except for summer at Lower Providence, Upper Providence, and Lower Bull stations) between average, wet, and dry years was statistically not significant (Table 2, one-way ANOVA, $p > 0.10$). The fraction of annual precipitation falling during the summer season was significantly higher (one-way ANOVA, $p < 0.10$) during the dry years as compared to wet years at Lower Providence, Upper Providence, and Lower Bull stations. In terms of air temperature, winter and spring temperatures were significantly warmer (one-way ANOVA, $p < 0.10$) during the dry years than those during wet years across all sites. There was no statistically significant difference (one-way ANOVA, $p > 0.10$) in fall season temperatures across all sites during average, wet, and dry years. However, wet year temperatures during summer at all four sites were significantly (one-way ANOVA, $p < 0.10$) colder than those during the average years.

Peak SWE was highly variable among the sites despite very similar precipitation regimes (Figure 2b). Consistent with an elevation influence, the recorded peak SWE was highest at Upper Bull. Although Lower Bull site is located at slightly higher elevation than Upper Providence and hence colder (Figure 3b), peak SWE was greater at the latter site across all years. A similar pattern was also observed between Lower Bull and Lower Providence during WYs 2009 and 2012 when recorded peak SWE was greater at the lower elevation site. These inconsistent patterns could be attributed to the differences in microclimate and energy exchange (Marks and Dozier, 1992). For example, although Lower Bull is at a higher elevation than Upper Providence and warmer by ~2°C in terms of mean monthly average temperature across all months (Figure 3b), the mean daily average maximum temperature over the snow accumulation season (January-March) was 0.40°C colder at the latter site ($p = 0.10$, Welch Two Sample t-test). Lower Bull meteorology site is dominated by rock outcrop, with very sparse vegetation in the surroundings, which

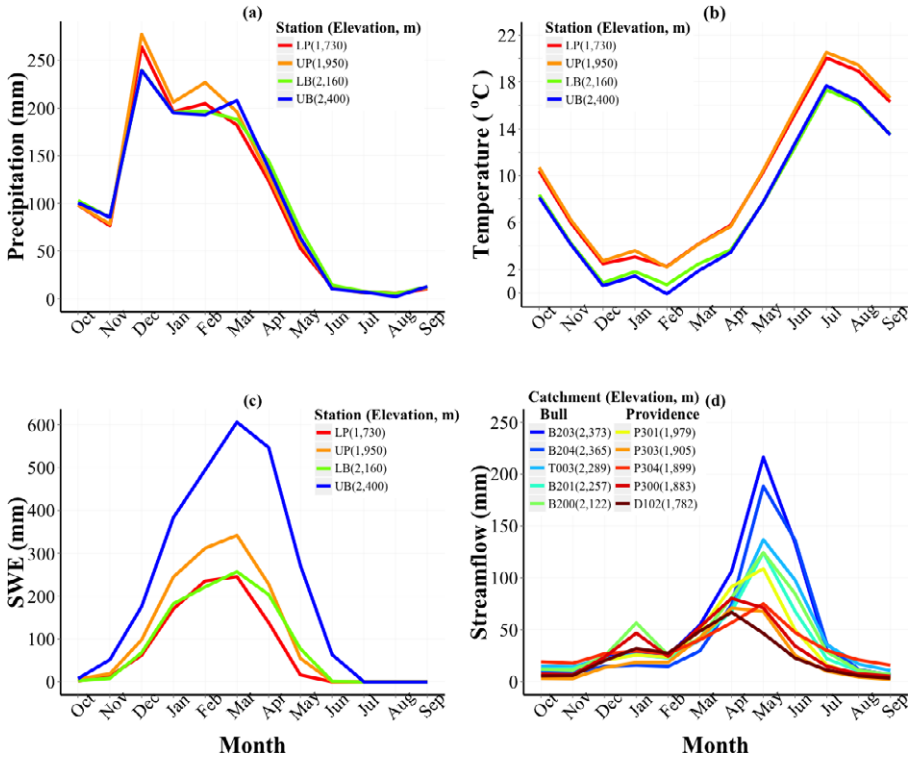

FIGURE 3. Monthly Average for All Years of Data: (a) Precipitation, (b) Mean Monthly Daily Average Air Temperature, (c) Snow Water Equivalent (SWE), and (d) Streamflow.

warms quickly when the sun is out and may have influenced the snow accumulation and melt.

Monthly average SWE at the four sites showed contrasting accumulation and melt patterns due to differences in elevation (Figure 3c). On average, timing and magnitude of peak SWE was very similar between Lower Providence and Lower Bull. However, snow disappeared faster at Lower Providence than Lower Bull; although this difference in snow disappearance date was statistically not significant (Figure 4f). Similarly, timing of snow disappearance was indistinguishable between Upper Providence and Lower Bull despite higher SWE at the former site. As compared to the other sites, average monthly SWE at Upper Bull was not only significantly higher but also lasted longer (Figure 4). On average, in spite of nearly identical precipitation amounts the number of snow-on-ground days was 138, 149, 157, and 204 days/year at Lower Providence, Upper Providence, Lower Bull, and Upper Bull, respectively (Figure 4e). Similarly, the average day of snow disappearance varied between 200 (18th April), 212 (30th April), 204 (22nd April), and 239 (27th May) days (starting from October 1) at Lower Providence, Upper Providence, Lower Bull, and Upper Bull, respectively.

The peak SWE to winter precipitation ratio ranged from 28 to 104% at Lower Providence, 36 to 109% at Upper Providence, 29 to 104% at Lower Bull, and 87 to 146% at Upper Bull across all observation years (Figure 4b). Over 100% peak SWE to winter precipitation ratio at some sites may be driven by early snowfall and rain on snow events during the fall season. We cannot reject the possibility of precipitation under-catch and snowdrift as alternative explanations for >100 peak SWE to winter precipitation ratio, especially at higher elevations where snowfall dominates over rainfall. Nonetheless, the peak SWE to winter precipitation ratio across sites was significantly higher at the Upper Bull site as compared to the other three sites. The differences in winter to annual precipitation ratio among the four sites were statistically not significant (Figure 4a). We found no strong correlation (Pearson's $0.08 \leq r \leq 0.45$) between total WY precipitation and peak SWE to winter precipitation ratio across all the sites. However, average air temperature showed strong negative correlation (Pearson's $-0.77 \leq r \leq -0.30$) with peak SWE to winter precipitation ratio (Figure 4). One exception was the Lower Bull site where temperature did not explain lower peak SWE to winter precipitation ratio, lower snow depth, fewer snow on the ground days, and earlier snow disappearance. This may be in part due to the differences in solar radiation, the largest source of energy contributor for snowmelt in the Sierra (Marks and Dozier, 1992), at the four sites.

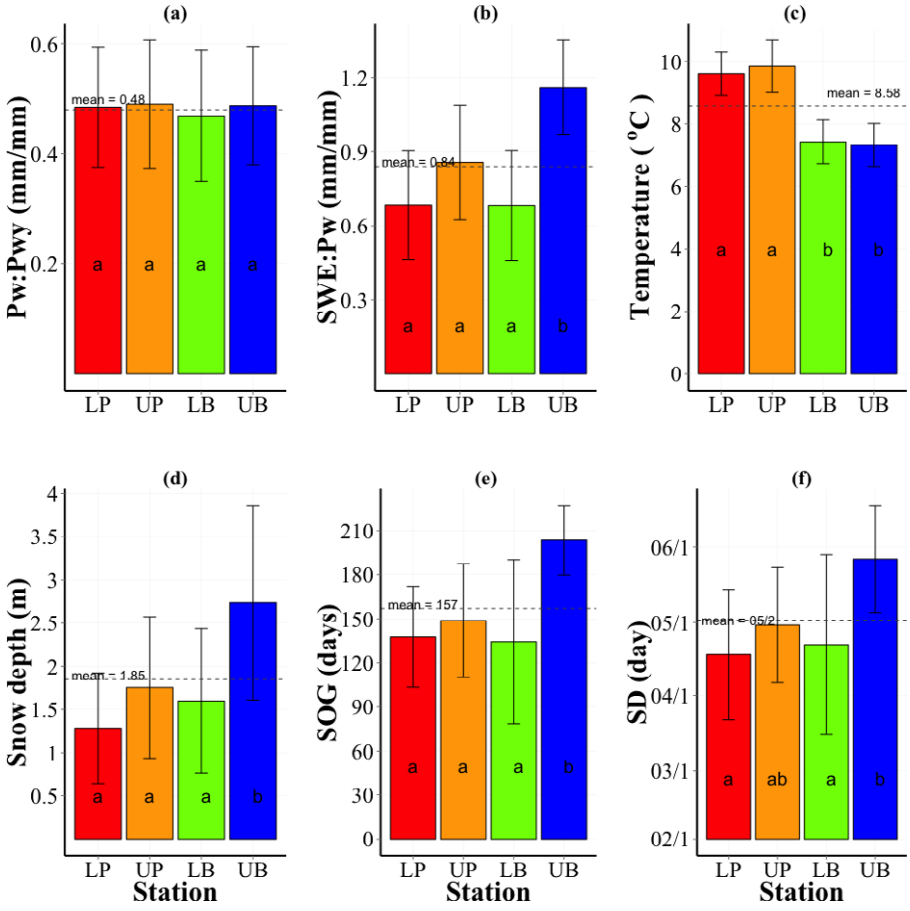

FIGURE 4. Variability in (a) Winter (Pw) to Water Year (Pwy) Precipitation Ratio, (b) Peak SWE (SWE) to Winter Precipitation (Pw) Ratio (%), (c) Average Daily Temperature, (d) Average Peak Snow Depth, (e) Number of Days Snow on Ground (SOG), and (f) Day of Snow Disappearance (SD) across the Four KREW Meteorological Stations. The bar graph shows the annual mean and error bar represents ± one standard deviation. The dotted horizontal lines show the mean value across the four stations. The same letters on the bar graph indicate statistically no significant differences between the stations (based on one-way ANOVA and post hoc Tukey's HSD tests, $p < 0.05$).

On average, Lower Bull (162 w/m^2) received higher incoming solar radiation (measured using CM3 Pyranometer, Kipp & Zonen, Inc., Delft, The Netherlands) than Lower Providence (160 w/m^2), Upper Providence (144 w/m^2), and Upper Bull (151 w/m^2).

Bull catchments, on average, had higher streamflow than the Providence catchments across all HSs (Table 3). In terms of flow seasonality, Bull catchments not only showed higher flow during winter months but also during the summer months (Figure 3d). One exception was P304, which showed highest Q_{min}, Q_5, Q_{25}, Q_{Fall}, and Q_{Summer} among all the catchments (Table 3). Additionally, the low pulse count was lower in P304 as compared to the rest of the catchments. Among the Providence catchments P301 consistently generated higher streamflow except during the dry years when P304 streamflow exceeded P301 (Figure 2c). Moreover, when a wet or above normal precipitation year was immediately followed by a dry or below normal precipitation year (*e.g.*, 2007 and 2012), P304 showed significantly higher streamflow than other Providence catchments, and was comparable to the Bull catchments (Figure 2c). This distinctive hydrologic behavior of P304 can be explained by relatively large groundwater storage as reflected by highest BFI, slowest flow recession (k), and gentlest FDC slope among all catchments (Table 3). In Providence, the centroid of flow timing (CT) was, on average, two weeks earlier than Bull. We found no systematic pattern in average stream dry days (DD) and high pulse count. On a seasonal time scale, the streamflow variability among different catchments was smaller during fall (σ = 12.5 mm), winter (σ = 17.8 mm), and summer (σ = 18.2 mm) than those in spring (σ = 108.1 mm).

Consistent with streamflow, Bull catchments along with P304 had the higher runoff ratio as compared to the other Providence catchments (Table 3). Irrespective of elevation, all catchments had a positive precipitation-intercept in the relationship between precipitation and discharge (Figure 5), which indicates that a minimum amount of precipitation is required to

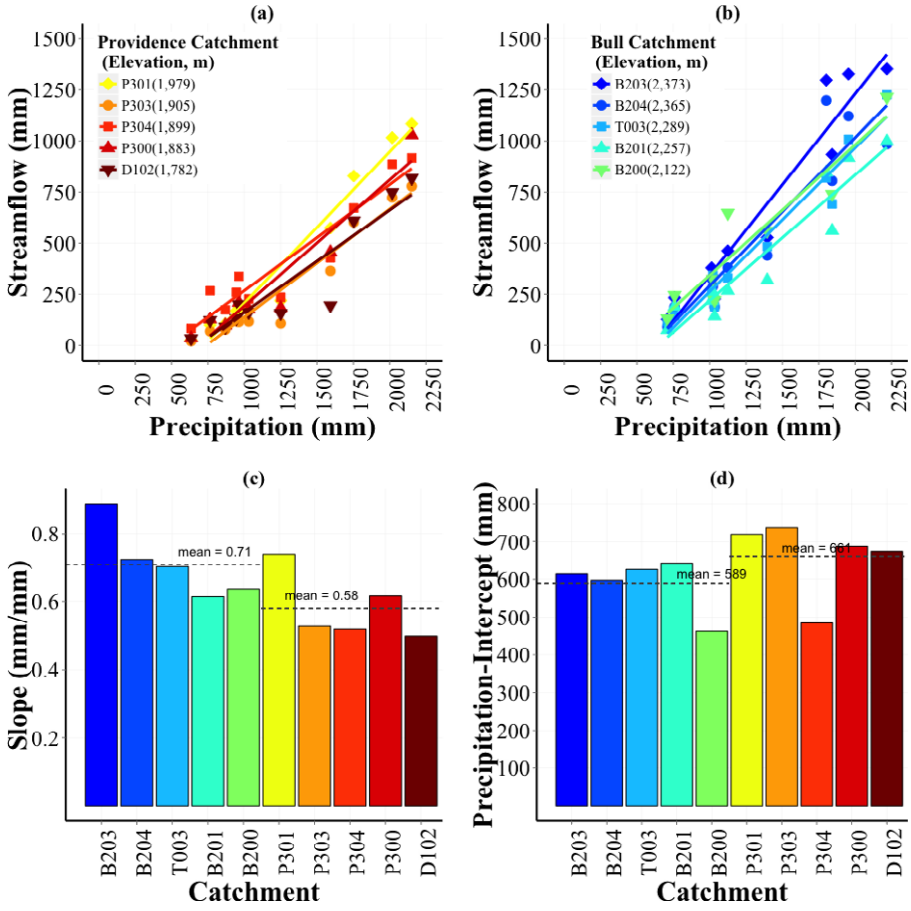

FIGURE 5. Annual Streamflow-Precipitation Relationship for (a) Providence and (b) Bull Catchments along with the Least Square Best Fit Line (c) Slope and (d) Precipitation-Intercept for Individual Catchments. The horizontal dotted lines on the bar plot show the mean value for Providence (yellow to brown colors) and Bull (blue to green colors) catchments separately.

generate any discharge. The mean precipitation threshold is slightly higher (661 mm) for Providence than Bull (589 mm) catchments but the difference was not statistically significant (p = 0.58, Welch Two Sample t-test). Catchment responsiveness to precipitation, as measured by the slope of P-Q relationship, was highly variable among different catchments with slope values significantly higher (p = 0.07, Welch Two Sample t-test) for Bull than for Providence catchments. Additionally, in all catchments average annual runoff ratio never exceeded the 50% threshold, indicating that the catchment discharge falls behind the catchment evapotranspiration (Table 3).

The relationships, as measured by the Pearson's correlation (r), between the PCDs and selected (Table 3) HSs are shown in Figure 6. It is worth mentioning that many of the PCDs are cross-correlated with each other. Catchment slope, aspect, drainage density, and NDVI showed negative correlation with elevation and may require disentangling the co-linearity of the system. Similarly, a positive cross-correlation exists between drainage area and relief. We, also found no significant correlation between HSs and catchment relief or aspect. Drainage area and catchment slope were only correlated with BFI and recession constant, respectively. Hence, for simplicity, we described the variability in HSs with respect to elevation and NDVI only. In the set of HSs used, BFI showed strong negative correlation ($r = -0.82$) with the drainage area (Figure 6). Runoff ratio, P-Q slope, and annual streamflow showed significant positive ($0.76 < r < 0.89$) and negative ($-0.87 < r < -0.75$) correlation with elevation and NDVI, respectively. There was a non-significant negative correlation ($r = -0.54$) between precipiation elasticity of streamflow (*i.e.*, ε_P) and elevation. Recession constant, was significantly correlated ($r = -0.61$) with catchment NDVI. Slope of the FDC and P-intercept showed no significant correlation with any of the PCDs.

The increase in annual streamflow as well as runoff ratio with elevation were further investigated by examining the rate of increase under various precipitation regimes (*i.e.*, average, wet, and dry years). On average, mean annual streamflow increased by 49 mm per 100 m increase in elevation (Figure 7a). This increase in streamflow with elevation was about four-fold higher in wet years (76 mm per 100 m

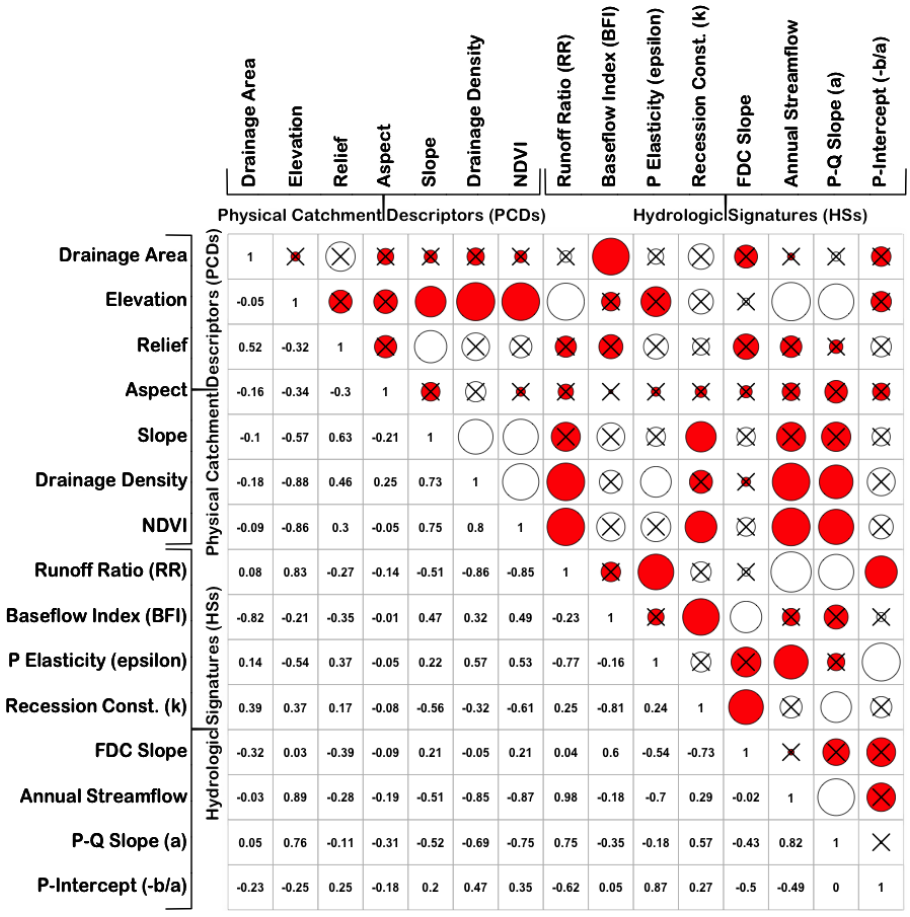

FIGURE 6. Correlation Matrix Showing the Dependence between Physical Catchment Descriptors (PCDs) and Hydrologic Signatures (HSs). The strength of the correlation is shown by the size of filled circles (positive: open circles and negative: filled red circles). The statistically significant ($p < 0.10$) correlations are marked with cross sign.

elevation gain) as compared to those during dry years (20 mm per 100 m elevation gain). Similarly, on average a 3% increase in runoff ratio (4% during wet years and 2% during dry years) was observed with 100 m increase in elevation (Figure 7b). The average increase in streamflow with elevation was very similar to that of the reduction in evapotranspiration with elevation (Figure 7c).

Overall, the selected HSs (Table 3) exhibited a strong variability, based on the ordination plot from the N-MDS analysis of Euclidian distances, in both space and time (Figure 8). Pairwise ANOSIM results indicated that both groups of HSs, catchment (*i.e.*, Providence and Bull) or climate (*i.e.*, average, wet and dry), were statistically dissimilar ($p < 0.01$). However, the degree of dissimilarity among the HSs due to variability in climate was higher than those due to variability in physical catchment characteristics between Providence and Bull. Although, the spread and overlap of descriptors were very similar between Providence and Bull catchments, N-MDS results show a slightly higher degree of dissimilarity for Bull than Providence (Figure 8a). In terms of climate, selected HSs during the average climate regime show significant overlap with wet and dry climate (Figure 8b). There was a high dissimilarity among HSs between wet and dry climate. Noticeably, irrespective of climate regime or catchment type, Providence catchment P304 (number 8 in Figure 8) stands out as an outlier. In terms of the ordination plot, there was very little overlap (*i.e.*, high degree of dissimilarity) of HSs from P304 with those from other catchments.

DISCUSSION

Catchment Similarity

In general, HSs showed considerable variability within Providence and Bull catchments and across the elevation gradient. Although climate variability

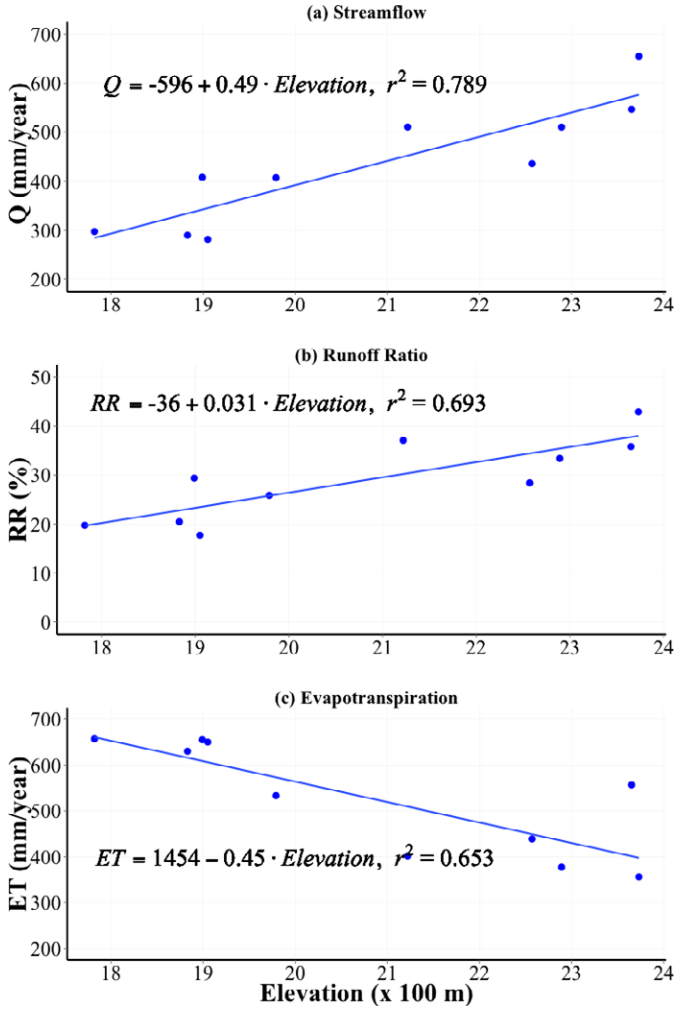

FIGURE 7. Elevation Dependence of Average Annual (a) Streamflow, (b) Runoff Ratio, and (c) Evapotranspiration.

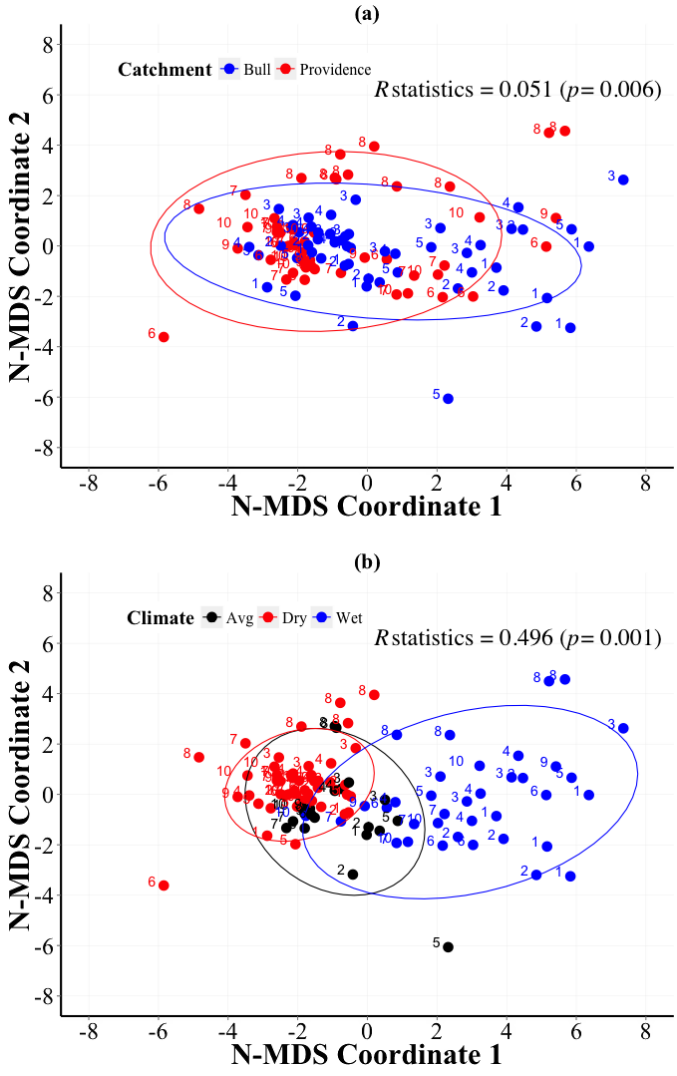

FIGURE 8. Nonparametric, multidimensional scaling (N-MDS) on Euclidian Distance (stress < 0.10) Showing the Degree of Similarity among the Descriptors of Hydrologic Signature across All the KREW Catchments and Water Years (2004-2014). The dissimilarity matrixes were calculated using the 18 hydrologic signatures listed in Table 2. Ellipses around each group of descriptors were drawn at 95% confidence level. Dots are identified by catchment with 1 (B203), 2 (B204), 3 (T003), 4 (B201), 5 (B200), 6 (P301), 7 (P303), 8 (P304), 9 (P300), and 10 (D102).

appears to be the first order control on dissimilarity of HSs, effects of small-scale differences in soil and subsurface flow characteristics on hydrologic functioning of these catchments cannot be ignored. For example, presence of slow recession and higher base flow in P304, which is climatologically similar to the other Providence catchments, mediated the HSs and separates the catchment into a different class that is distinct from both Providence and Bull catchments (Table 3, Figure 8). This unique hydrologic functioning of P304 as reflected by slow recession and higher base flow and other metrics can be attributed to several factors. The channel is narrow and the stream has not downcut to reach a bedrock base, as have most of our other KREW streams in places, which may enhance base flow. Also, the percent of rock in the coarse soil (particle size > 2 mm) is significantly lower (<20%) for P304 as compared to other Providence catchments (30-50%) and may lead to differences in the hydraulic conductivity. The slower recession and high base flow in P304 can also be attributed to a small man-made dam upstream of the weir, which became a meadow over time. Nonetheless, these small-scale catchment soil and geologic differences may play a bigger role on some HSs than others (Table 3). Therefore, interpretation of HSs in the context of forest management or any other form of landscape disturbance (*e.g.*, tree mortality and fire) based on spatial proximity or grouping could be misleading. Also, the choice and selection of HSs could be the key in interpreting the hydrologic impact of landscape disturbances.

Increase in Streamflow with Elevation

As noted by Hunsaker *et al.* (2012), increase in streamflow with elevation, despite similar precipitation, can be explained by higher precipitation falling as snow, lower sublimation, and decline in evapotranspiration with increasing catchment elevation. The higher elevation catchments are more energy limited as compared to lower elevation catchments leading to higher snow fraction and a shorter growing season (Goulden *et al.*, 2012; Goulden and Bales, 2014). As evident from the higher SWE/Pw ratio at Upper Bull (Figure 4b), the sublimation losses are limited at high elevations due to colder temperatures. Additionally, the soil is less developed and drains rapidly in high elevation catchments. Hence, despite the fact that snow stays longer at higher elevations, and thus the melt water is available for plant use, the average evapotranspiration declines rapidly above 2,000 m elevation (Lundquist and Loheide, 2011; Goulden *et al.*, 2012). In KREW, average evapotranspiration is 32% lower in upper elevation (>2,000 m) Bull catchments as compared to lower elevation (<2,000) Providence catchments. Using the empirical relationship between NDVI and evapotranspiration developed by Goulden *et al.* (2012), we estimated a decline of evapotranspiration in KREW catchments by 45 mm per 100-m elevation gain (Figure 7c). This rate of evapotranspiration decline with elevation is slightly lower than the rate of streamflow increase with elevation (*i.e.*, 49 mm per 100-m elevation gain).

The snow fraction (percentage of the total precipitation in each year falling as snow) in the Sierra Nevada, which increases with increasing elevation, is highly sensitive to changes in temperature. Safeeq *et al.* (2015b) state a 10% decrease in snow fraction for every 1°C rise in temperature. As temperatures warm, a decline in annual snow fraction has been shown to cause a decline in streamflow. Berghuijs *et al.* (2014) showed 0.37 mm/mm on average increase in precipitation-normalized streamflow to a unit increase in snow fraction. For the KREW, if we ignore the uncertainty associated with the empirically derived evapotranspiration, the additional (4 mm per 100-m elevation gain) increase of streamflow can be solely attributed to a proportionally higher snow to precipitation ratio. On average the peak SWE to precipitation ratio among the four KREW meteorological stations increased by 3% per 100-m elevation gain (R^2 = 0.5). This increase in peak SWE/precipitation ratio with elevation, mainly attributed to greater proportion of precipitation falling as snow and lower sublimation, is rather small and alone cannot explain the increase in streamflow with elevation (Figure 7). Reduced evapotranspiration with elevation, both in response to shorter growing season and lower NDVI (declines by: 0.04/100 m elevation gain, R^2 = 0.73), seems to be a primary factor in regulating streamflow. Hence, any further decline in snow fraction under a warmer climate and its effect on streamflow will likely be driven by the response of evapotranspiration with reduced snow cover and the associated feedbacks. As predicted by numerical models in the Sierra Nevada, less snow, higher sublimation, and earlier snowmelt with a warmer climate will increase forest water stress and reduce net primary productivity (Tague *et al.*, 2009; Tague and Peng, 2013). If these model (*i.e.*, Tague *et al.*, 2009; Tague and Peng, 2013) results hold true, then the forests may be most affected by the reduced snow fraction scenario.

Patterns of Precipitation Elasticity Streamflow (ε_P) between Providence and Bull Catchments

Consistent with previous findings (Chiew, 2006; Zheng *et al.*, 2009), we report an inverse relationship between the precipitation elasticity of streamflow and catchment runoff ratio (Figure 6). However, the spatial pattern of ε_P reveals significant differences between the Providence and Bull catchments. With the exception of P304, the catchment with the highest groundwater influence (Table 3), all Providence catchments show significantly (p = 0.004, Welch Two Sample t-test) higher ε_P as compared to Bull catchments. This indicates that despite the deeper soil and higher soil water storage in lower elevation catchments (Bales *et al.*, 2015) the proportional change in annual streamflow is more dependent on proportional change in annual precipitation. In contrast, the proportional change in annual streamflow with respect to proportional change in annual precipitation (*i.e.*, ε_P) in the higher elevation Bull catchments is very similar to a groundwater dominated catchment (*i.e.*, P304). This lower value of ε_P in high elevation catchments, despite a lack of subsurface storage due to shallow soils, can be attributed to delayed snowmelt and lower evapotranspiration. Both delayed snowmelt and lower evapotranspiration can enhance the carryover storage and increase the streamflow persistence in the following year. However, earlier snowmelt and higher evapotranspiration limits the carryover storage in Providence catchments (with the exception of P304) despite the deeper soil with a higher potential for subsurface water storage.

The role of delayed snowmelt and lower evapotranspiration in buffering the streamflow sensitivity to precipitation, as evident from ε_P in high elevation Bull catchments, are likely to change in the future. Under warmer climate with reduced snowpack, earlier melt, and increased evapotranspiration these

high elevation catchments with shallow soil may likely lose their ability to carryover storage and buffer subsequent year streamflow. In fact, because of shallow soils these high elevation catchments may show greater stress to climate warming than lower elevation catchments, especially if changes in snowpack are driven by both higher temperatures and reduced precipitation (Pierce and Cayan, 2013; Goulden and Bales, 2014). These empirical inferences are consistent with results from numerical modeling showing increased drought stress under a warming climate in snow dominated catchments (Tague and Peng, 2013).

Water is stored or moves between only a few compartments of the forest ecosystem: soil, surface water, vegetation, groundwater, and the atmosphere. In addition to direct evaporation/sublimation, under similar climate and hydrologic conditions the amount and type of vegetation governs how much surface and soil water is transpired to the atmosphere and thus reduced in these compartments. Tree and shrub densities in the Sierra Nevada are very high for various reasons including 80 or more years of fire suppression and 40 years of challenges during planning and implementing mechanical thinning and/or timber harvest projects (*Long et al.*, 2014). Multiple stressors affect the health of southern Sierra Nevada forests: air pollution, the density of the vegetation, and low precipitation years. The only one of these stressors that forest management can directly influence is the amount and type of vegetation on the land through timber harvesting, mechanical forest thinning, and prescribed fire. These management activities can improve forest health and possibly increase water yield from forest streams (Bales *et al.*, 2011; Robles *et al.*, 2014; Saksa, 2015). However, responsible management needs to balance multiple ecosystem services such as water quality and quantity, wildlife habitat, vegetation diversity and condition, and recreational use (Long *et al.*, 2014). Prior to the establishment of KREW there was very little data on the variability of water quantity and quality in headwater streams of the Sierra Nevada, and thus little information to guide forest managers in the design of management treatments to benefit ecosystems and humans (Hunsaker *et al.*, 2014).

CONCLUSIONS

Evaluations of streamflow-based HSs were performed in 10 southern Sierra Nevada catchments with the goal of describing their hydrologic functioning and informing forest management. In general, temporal variability in climate exerts first order control on the functioning of these catchments, respectively. However, in some cases the small-scale variability in soil and geologic characteristics may buffer against climate variability (*e.g.*, catchment P304). We find an increase in streamflow by elevation that is closely matched by the decline in evapotranspiration with increasing elevation. The effect of increasing snowfall ratio (with elevation) on streamflow (Figure 4) was much lower than previously reported by Berghuijs *et al.* (2014). However, the presence of snowpack that melts late in the season, reduced evapotranspiration due to lower vegetation density (Table 1), and shorter growing season may mediate the streamflow sensitivity to precipitation (*i.e.*, ε_P) through carryover storage even in the absence of deeper soil. While it is still unclear how evapotranspiration will respond to warming temperature (Goulden and Bales, 2014) and reduced snowpack in these catchments, reduction in snowpack magnitude and earlier shift in timing will likely undermine the streamflow persistence by reducing the carryover storage.

About 50-60% of California's surface water comes from the Sierra Nevada, and a high proportion of this water comes from forested headwater streams (first through third order streams). Thus forest vegetation in the mountains plays an important role in California's water supply. The 10 years of data presented here include a sampling of wet, dry, and average water years; thus for the first time, we can observe how first through third order streams respond to these highly variable weather conditions in the Sierra Nevada. KREW takes measurements on 10 streams in two groups, to improve robustness of the sample size for a landscape study. A better understanding of how similar (or different) adjacent and hierarchical catchments behave under varying weather conditions helps scientists know how reliable extrapolations can be to local, regional, and national headwater systems with similar soils, topography, and climate. Also, the two watershed groups at KREW span the current rain-snow transition zone, which makes these findings useful for climate change investigations in the Sierra Nevada and elsewhere. These detailed data also are extremely useful for modeling exercises of climate change and forest density, and several modeling efforts are in progress.

ACKNOWLEDGMENTS

Many people have been critical to the success of this long-term research so we can't possibly mention everyone here. Sean Eagan and Jeff Anderson were the hydrologists who designed and installed most instruments at KREW; Thomas Whitaker was the hydrologist who helped Dr. Hunsaker run KREW after Mr. Eagan

left; and more recently KREW has been kept functional by Kevin Mazzocco and Amber Olsson (PSW technicians) and Jason Smith (UC Merced technician). Matt Stuemky is appreciated for his GIS and database work over the years. KREW was established with USDA Forest Service funding from the National Fire Plan and consistently supported by the Pacific Southwest Research Station. Some support since 2007 also has been provided through the Southern Sierra Critical Zone Observatory (National Science Foundation EAR-0725097). Use of firm or trade names is for reader information only and does not imply endorsement of any product or service by the U.S. Government.

LITERATURE CITED

Andréassian, V., 2004. Waters and Forests: From Historical Controversy to Scientific Debate. Journal of Hydrology 291(1): 1-27.

Arismendi, I., S.L. Johnson, J.B. Dunham, and R. Haggerty, 2013. Descriptors of Natural Thermal Regimes in Streams and Their Responsiveness to Change in the Pacific Northwest of North America. Freshwater Biology 58(5):880-894.

Arnold, J. and P. Allen, 1999. Automated Methods for Estimating Base-Flow and Ground Water Recharge from Streamflow Records. Journal of the American Water Resources Association 35:411-424.

Arnold, J., P. Allen, R. Muttiah, and G. Bernhardt, 1995. Automated Base Flow Separation and Recession Analysis Techniques. Ground Water 33:1010-1018.

Baker, D.B., R.P. Richards, T.T. Loftus, and J.W. Kramer, 2004. A New Flashiness Index: Characteristics and Applications to Midwestern Rivers and Streams. Journal of the American Water Resources Association 40(2):503-522.

Bales, R.C., J.J. Battles, Y. Chen, M.H. Conklin, E. Holst, K.L. O'Hara, P. Saksa, and W. Stewart, 2011. Forests and Water in the Sierra Nevada: Sierra Nevada Watershed Ecosystem Enhancement Project. Sierra Nevada Research Institute Report. www.ucanr.edu/sites/cff/files/146199.pdf, *accessed* February 2016.

Bales, R.C., M.L. Goulden, C.T. Hunsaker, M.H. Conklin, P.C. Hartsough, A.T. O'Geen, J. Hopmans, and M. Safeeq, 2015. Drought Effects on Evapotranspiration and Subsurface Water Storage in the Southern Sierra Nevada. Abstract H33M-06 presented at 2015 Fall Meeting, AGU, San Francisco, California, December 14–18.

Berghuijs, W.R., R.A. Woods, and M. Hrachowitz, 2014. A Precipitation Shift from Snow Towards Rain Leads to a Decrease in Streamflow. Nature Climate Change 4(7):583-586.

Biederman, J.A., A.A. Harpold, D.J. Gochis, B.E. Ewers, D.E. Reed, S.A. Papuga, and P.D. Brooks, 2014. Increased Evaporation Following Widespread Tree Mortality Limits Streamflow Response. Water Resources Research 50(7):5395-5409.

Biederman, J.A., A.J. Somor, A.A. Harpold, E.D. Gutmann, D.D. Breshears, P.A. Troch, D.J. Gochis, R.L. Scott, A.J.H. Meddens, and P.D. Brooks, 2015. Recent Tree Die-Off Has Little Effect on Streamflow in Contrast to Expected Increases from Historical Studies. Water Resources Research 51(12):9775-9789.

Bosch, J.M. and J.D. Hewlett, 1982. A Review of Catchment Experiments to Determine the Effect of Vegetation Changes on Water Yield and Evapotranspiration. Journal of Hydrology 55:2-23.

Brown, A.E., L. Zhang, T.A. McMahon, A.W. Western, and R.A. Vertessy, 2005. A Review of Paired Catchment Studies for Determining Changes in Water Yield Resulting from Alterations in Vegetation. Journal of Hydrology 310(1):28-61.

Chiew, F.H.S., 2006. Estimation of Rainfall Elasticity of Streamflow in Australia. Hydrological Sciences Journal 51(4):613-625.

Daly, C., R.P. Neilson, and D.L. Phillips, 1994. A Statistical-Topographic Model for Mapping Climatological Precipitation over Mountainous Terrain. Journal of Applied Meteorology 33: 140-158.

Eckhardt, K., 2005. How to Construct Recursive Digital Filters for Baseflow Separation. Hydrological Processes 19:507-515.

Frassetto, A.M., G. Zandt, H. Gilbert, T.J. Owens, and C.H. Jones, 2011. Structure of the Sierra Nevada from Receiver Functions and Implications for Lithospheric Foundering. Geosphere 7 (4):898-921.

Fu, G., S.P. Charles, and F.H. Chiew, 2007. A Two-Parameter Climate Elasticity of Streamflow Index to Assess Climate Change Effects on Annual Streamflow. Water Resources Research 43, W11419, DOI: 10.1029/2007WR005890.

Goulden, M.L., R.G. Anderson, R.C. Bales, A.E. Kelly, M. Meadows, and G.C. Winston, 2012. Evapotranspiration Along an Elevation Gradient in the Sierra Nevada. Journal of Geophysical Research 117, G03028, DOI: 10.1029/2012JG002027.

Goulden, M.L. and R.C. Bales, 2014. Mountain Runoff Vulnerability to Increased Evapotranspiration with Vegetation Expansion. Proceedings of the National Academy of Sciences 111(39):14071-14075, DOI: 10.1073/pnas.1319316111.

Grant, G.E., C.L. Tague, and C.D. Allen, 2013. Watering the Forest for the Trees: An Emerging Priority for Managing Water in Forest Landscapes. Frontiers in Ecology and the Environment 11 (6):314-321.

Hamlet, A.F. and D.P. Lettenmaier, 2007. Effects of 20th Century Warming and Climate Variability on Flood Risk in the Western U.S. Water Resources Research 43, W06427, DOI: 10.1029/2006WR005099.

Hamlet, A.F., P.W. Mote, M.P. Clark, and D.P. Lettenmaier, 2005. Effects of Temperature and Precipitation Variability on Snowpack Trends in the Western United States. Journal of Climate 18(21):4545-4561.

Harpold, A., P. Brooks, S. Rajagopal, I. Heidbuchel, A. Jardine, and C. Stielstra, 2012. Changes in Snowpack Accumulation and Ablation in the Intermountain West. Water Resources Research 48, W11501, DOI: 10.1029/2012WR011949.

Hunsaker, C.T., J. Adair, J. Auman, K. Weidick, and T. Whitaker, 2007. Kings River Experimental Watershed Research Study Plan. http://www.fs.fed.us/psw/topics/water/kingsriver/documents/miscellaneous/KREW_Study_Plan_Sept2007.pdf, *accessed* March 2016.

Hunsaker, C.T., J.W. Long, and D.B. Herbst, 2014. Watershed and Stream Ecosystems. *In*: Science Synthesis to Support Socioecological Resilience in the Sierra Nevada and Southern Cascade Range. General Technical Report PSW-GTR-247, Vol. 1. J.W. Long, L. Quinn-Davidson, and C.N. Skinner (Editors). U.S. Department of Agriculture, Forest Service, Pacific Southwest Research Station, Albany, California, pp. 265-322.

Hunsaker, C.T., T.W. Whitaker, and R.C. Bales, 2012. Snowmelt Runoff and Water Yield along Elevation and Temperature Gradients in California's Southern Sierra Nevada. Journal of the American Water Resources Association 48:667-678, DOI: 10.1111/j.1752-1688.2012.00641.x.

Institute of Hydrology, 1980a. Research Report, Volume 1 of Low Flow Studies. Institute of Hydrology, Wallingford, United Kingdom, 42 pp.

Institute of Hydrology, 1980b. Catchment Characteristic Estimation Manual, Volume 3 of Low Flow Studies. Institute of Hydrology, Wallingford, United Kingdom, 27 pp.

Johnson, D.W., C.T. Hunsaker, D.W. Glass, B.M. Rau, and B.A. Roath, 2011. Carbon and Nutrient Contents in Soils from the Kings River Experimental Watersheds, Sierra Nevada Mountains, California. Geoderma 160:490-502.

Jones, J.A., G.L. Achterman, L.A. Augustine, I.F. Creed, P.F. Ffolliott, L. MacDonald, and B.C. Wemple, 2009. Hydrologic Effects of a Changing Forested Landscape—Challenges for

the Hydrological Sciences. Hydrological Processes 23(18):2699-2704.

Kadioglu, M. and Z. Sen, 2001. Monthly Precipitation-Runoff Polygons and Mean Runoff Coefficients. Hydrological Sciences Journal 46(1):3-11.

Klos, P.Z., T.E. Link, and J.T. Abatzoglou, 2014. Extent of the Rain-Snow Transition Zone in the Western US under Historic and Projected Climate. Geophysical Research Letters 41 (13):4560-4568.

Knowles, N., M.D. Dettinger, and D.R. Cayan, 2006. Trends in Snowfall Versus Rainfall in the Western United States. Journal of Climate 19:4545-4559.

Kroll, C., J. Luz, B. Allen, and R.M. Vogel, 2004. Developing a Watershed Characteristics Database to Improve Low Streamflow Prediction. Journal of Hydrologic Engineering 9(2):116-125.

Kruskal, J.B., 1964. Nonmetric Multidimensional Scaling: A Numerical Method. Psychometrika 29:115-129.

Long, J.W., L. Quinn-Davidson, and C.N. Skinner, 2014. Science Synthesis to Support Socioecological Resilience in the Sierra Nevada and Southern Cascade Range. General Technical Report PSW-GTR-247, 712 pp., U.S. Department of Agriculture, Forest Service, Pacific Southwest Research Station, Albany, California.

Luce, C.H. and Z.A. Holden, 2009. Declining Annual Streamflow Distributions in the Pacific Northwest United States, 1948-2006. Geophysical Research Letters 36, L16401, DOI: 10.1029/2009GL039407.

Lundquist, J.D. and S.P. Loheide, 2011. How Evaporative Water Losses Vary between Wet and Dry Water Years as a Function of Elevation in the Sierra Nevada, California, and Critical Factors for Modeling. Water Resources Research 47:1-13, DOI: 10.1029/2010WR010050.

Marks, D. and J. Dozier, 1992. Climate and Energy Exchange at the Snow Surface in the Alpine Region of the Sierra Nevada. 2. Snow Cover Energy Balance. Water Resources Research 28 (11):3043-3054.

Maurer, E.P., I.T. Stewart, C. Bonfils, P.B. Duffy, and D. Cayan, 2007. Detection, Attribution, and Sensitivity of Trends Toward Earlier Streamflow in the Sierra Nevada. Journal of Geophysical Research 112, D11118, DOI: 10.1029/2006JD008088.

Mayer, T.D. and S.W. Naman, 2011. Streamflow Response to Climate as Influenced by Geology and Elevation. Journal of the American Water Resources Association 47(4):724-738.

Miller, M.P., H.M. Johnson, D.D. Susong, and D.M. Wolock, 2015. A New Approach for Continuous Estimation of Baseflow Using Discrete Water Quality Data: Method Description and Comparison with Baseflow Estimates from Two Existing Approaches. Journal of Hydrology 522:203-210.

Mote, P.W., A.F. Hamlet, M.P. Clark, and D.P. Lettenmaier, 2005. Declining Mountain Snowpack in Western North America. Bulletin of the American Meteorological Society 86(1):39-49.

Olden, J.D. and N.L. Poff, 2003. Redundancy and the Choice of Hydrologic Indices for Characterizing Streamflow Regimes. River Research and Applications 19:101-121.

Parrish, J.G., 2006. Simplified Geologic Map of California: California Geological Survey Map Sheet 57. http://www.conservation.ca.gov/cgs/information/publications/ms/Documents/MS057.pdf, *accessed* April 2015.

Pierce, D.W. and D.R. Cayan, 2013. The Uneven Response of Different Snow Measures to Human-Induced Climate Warming. Journal of Climate 26:4148-4167.

Posavec, K., A. Bačani, and Z. Nakić, 2006. A Visual Basic Spreadsheet Macro for Recession Curve Analysis. Ground Water 44 (5):764-767.

Robles, M.D., R.M. Marshall, F. O'Donnell, E.B. Smith, J.A. Haney, and D.F. Gori, 2014. Effects of Climate Variability and Accelerated Forest Thinning on Watershed-Scale Runoff in Southwestern USA Ponderosa Pine Forests. PLoS ONE 9(10): e111092, DOI: 10.1371/journal.pone.0111092.

Safeeq, M. and A. Fares, 2012. Hydrologic Response of a Hawaiian Watershed to Future Climate Change Scenarios. Hydrological Processes 26(18):2745–2764.

Safeeq, M., G.E. Grant, S.L. Lewis, M.G. Kramer, and B. Staab, 2014. A Hydrogeologic Framework for Characterizing Summer Streamflow Sensitivity to Climate Warming in the Pacific Northwest, USA. Hydrology and Earth System Sciences 18 (9):3693-3710.

Safeeq, M., G.E. Grant, S.L. Lewis, and B. Staab, 2015a. Predicting Landscape Sensitivity to Present and Future Floods in the Pacific Northwest, USA. Hydrological Processes 29(26):5337-5353.

Safeeq, M., G.E. Grant, S.L. Lewis, and C. Tague, 2013. Coupling Snowpack and Groundwater Dynamics to Interpret Historical Streamflow Trends in the Western United States. Hydrological Processes 27(5):655-668.

Safeeq, M., S. Shukla, I. Arismendi, G.E. Grant, S.L. Lewis, and A. Nolin, 2015b. Influence of Winter Season Climate Variability on Snow-Precipitation Ratio in the Western United States. International Journal of Climatology 36(9):3175-3190, DOI: 10.1002/joc.4545.

Saksa, P., 2015. Forest Management, Wildfire, and Climate Impacts on the Hydrology of Sierra Nevada Mixed-Conifer Watersheds. Ph.D. Dissertation, University of California, Merced.

Sankarasubramanian, A., R.M. Vogel, and J.F. Limbrunner, 2001. Climate Elasticity of Streamflow in the United States. Water Resources Research 37:1771-1781.

Sawicz, K., T. Wagener, M. Sivapalan, P. Troch, and G. Carrillo, 2011. Catchment Classification: Empirical Analysis of Hydrologic Similarity Based on Catchment Function in the Eastern USA. Hydrology and Earth System Sciences 15(9):2895-2911.

Schaake, J.C., 1990. From Climate to Flow, Climate Change and US Water Resources, P.E. Waggoner (Editor). John Wiley & Sons, New York, pp. 177-206.

Smakhtin, V.U., 2001. Low Flow Hydrology: A Review. Journal of Hydrology 240:147-186.

Soil Survey Staff, 2015. Natural Resources Conservation Service, United States Department of Agriculture. U.S. General Soil Map (STATSGO2). http://sdmdataaccess.nrcs.usda.gov/, *accessed* April 2015.

Stednick, J.D., 1996. Monitoring the Effects of Timber Harvest on Annual Water Yield. Journal of Hydrology 176:79-95.

Stewart, I.T., D.R. Cayan, and M.D. Dettinger, 2005. Changes Toward Earlier Streamflow Timing across Western North America. Journal of Climate 18(8):1136-1155.

Sujono, J., S. Shikasho, and K. Hiramatsu, 2004. A Comparison of Techniques for Hydrograph Recession Analysis. Hydrological Processes 18(3):403-413.

Tague, C. and G.E. Grant, 2009. Groundwater Dynamics Mediate Low-Flow Response to Global Warming in Snow-Dominated Alpine Regions. Water Resources Research 45, W07421, DOI: 10.1029/2008WR007179.

Tague, C. and H. Peng, 2013. The Sensitivity of Forest Water Use to the Timing of Precipitation and Snowmelt Recharge in the California Sierra: Implications for a Warming Climate. Journal of Geophysical Ressearch: Biogeoscience 118(2):875-887, DOI: 10.1002/jgrg.20073.

Tague, C., L. Seaby, and A. Hope, 2009. Modeling the Eco-Hydrologic Response of a Mediterranean Type Ecosystem to the Combined Impacts of Projected Climate Change and Altered Fire Frequencies. Climatic Change 93(1-2):137-155.

Tallaksen, L.M., 1995. A Review of Baseflow Recession Analysis. Journal of Hydrology 165(1-4):349-370.

Tohver, I.M., A.F. Hamlet, and S.Y. Lee, 2014. Impacts of 21st-Century Climate Change on Hydrologic Extremes in the Pacific

Northwest Region of North America. Journal of the American Water Resources Association 50(6):1461-1476.

Troendle, C.A., L.H. MacDonald, C.H. Luce, and I.J. Larsen, 2010. Fuel Management and Water Yield. *In*: Cumulative Watershed Effects of Fuel Management in the Western United States, General Technical Report RMRS-GTR-231, W.J. Elliot, I.S. Miller, and L. Audin (Editors). United States Department of Agriculture, Forest Service, Rocky Mountain Research Station, Fort Collins, Colorado, pp. 126-148.

Vogel, R.M. and C.N. Kroll, 1992. Regional Geohydrologic-Geomorphic Relationships for the Estimation of Low-Flow Statistics. Water Resources Research 28:2451-2458.

Vogel, R.M. and C.N. Kroll, 1996. Estimation of Baseflow Recession Constants. Water Resources Management 10:303-320.

Wahl, K.L. and T.L. Wahl, 1988. Effects of Regional Ground-Water Declines on Streamflows in the Oklahoma Panhandle. *In*: Proceedings of Symposium on Water-Use Data for Water Resources Management, M. Waterstone and R.J. Burt (Editors). American Water Resources Association, Tucson, Arizona, pp. 239-249.

Wahl, K.L. and T.L. Wahl, 1995. Determining the Flow of Comal Springs at New Braunfels, Texas. Proceedings of Texas Water '95, August 16-17, 1995. American Society of Civil Engineers, San Antonio, Texas, pp. 77-86.

Wolock, D.M., 2003. Estimated Mean Annual Natural Ground-Water Recharge in the Conterminous United States (No. 2003-311).

Yadav, M., T. Wagener, and H. Gupta, 2007. Regionalization of Constraints on Expected Watershed Response Behavior for Improved Predictions in Ungauged Basins. Advances in Water Resources 30(8):1756-1774.

Zhang, Z., T. Wagener, P. Reed, and R. Bhushan, 2008. Reducing Uncertainty in Predictions in Ungauged Basins by Combining Hydrologic Indices Regionalization and Multiobjective Optimization, Water Resources Research 44, W00B04, DOI: 10.1029/2008WR006833.

Zhao, F., L. Zhang, Z. Xu, and D.F. Scott, 2010. Evaluation of Methods for Estimating the Effects of Vegetation Change and Climate Variability on Streamflow. Water Resources Research 46, W03505, DOI: 10.1029/2009WR007702.

Zheng, H., L. Zhang, R. Zhu, C. Liu, Y. Sato, and Y. Fukushima, 2009. Responses of Streamflow to Climate and Land Surface Change in the Headwaters of the Yellow River Basin. Water Resources Research 45, W00A19, DOI: 10.1029/2007WR006665.